Space-Time Adaptive MMSE Multiuser Decision Feedback Detectors With Multiple-Feedback Interference Cancellation for CDMA Systems

Yunlong Cai and Rodrigo C. de Lamare, *Member, IEEE*

***Abstract*—In this paper, we propose a novel space-time minimum mean square error (MMSE) decision feedback (DF) detection scheme for direct-sequence code-division multiple access (DS-CDMA) systems with multiple receive antennas, which employs multiple-parallel-feedback (MPF) branches for interference cancellation. The proposed space-time receiver is then further combined with cascaded DF stages to mitigate the deleterious effects of error propagation for uncoded schemes. To adjust the parameters of the receiver, we also present modified adaptive stochastic gradient (SG) and recursive least squares (RLS) algorithms that automatically switch to the best-available interference cancellation feedback branch and jointly estimate the feedforward and feedback filters. The performance of the system with beamforming and diversity configurations is also considered. Simulation results for an uplink scenario with uncoded systems show that the proposed space-time MPF-DF detector outperforms existing schemes such as linear, parallel DF (P-DF), and successive DF (S-DF) receivers in terms of bit error rate (BER) and achieves a substantial capacity increase in terms of the number of users, compared with the existing schemes. We also derive the expressions for MMSE achieved by the analyzed DF structures, including the novel scheme, with imperfect and perfect feedback and expressions of signal-to-interference-plus-noise ratio (SINR) for the beamforming and diversity configurations with linear receivers.**

***Index Terms*—Antenna arrays, decision feedback (DF), direct-sequence code-division multiple access (DS-CDMA), interference suppression, multiuser detection.**

I. Introduction

In direct-sequence code-division multiple-access (DS-CDMA) systems, substantial work has been devoted to the design of schemes for interference mitigation. The major source of interference in most code-division multiple-access (CDMA) systems is multiaccess interference (MAI), which arises due to the fact that users communicate through the same physical channel with nonorthogonal signals. Multiuser detection has been proposed as a means to suppress MAI, increasing the capacity and performance of CDMA systems [1], [2]. The optimal multiuser detector of Verdu [3] suffers from exponential complexity and requires the knowledge of timing, amplitude, and signature sequences for all users. This fact has motivated the development of various suboptimal strategies with affordable complexity: the linear [4] and decision feedback (DF) [5] receivers, the successive interference canceller [6], and the multistage detector [7]. For uplink scenarios, some works [8], [13] have shown that DF structures, which are relatively simple and perform linear interference suppression, followed by interference cancellation, provide substantial gains over linear detection.

Among these schemes, the minimum mean square error (MMSE) multiuser DF detectors have emerged as highly effective solutions for the uplink as they provide effective MAI suppression, significant capacity increase, and excellent performance, compared with related detectors [9]–[14], at a relatively modest complexity. In particular, when using short or repeated spreading sequences, the MMSE design criterion leads to adaptive versions, which only require a training sequence to estimate the receiver parameters. The work of Honig and Woodward [10] has shown that the design of adaptive DF receivers based on the MMSE criterion using basic DF structures, i.e., the successive DF (S-DF) and the parallel DF (P-DF) schemes, can provide substantial gains over linear schemes. Both S-DF and P-DF schemes have their limitations: However, the P-DF scheme, which is more sensitive to error propagation than the S-DF, provides relatively better performance. The works in [9] and [10], however, did not consider the incorporation of antenna arrays. Adaptive space-time DF detectors were proposed by Smee and Schwartz [11], although the work was limited to the use of adaptive algorithms for only the feedforward filter with S-DF structures. Another technique that can substantially increase the capacity of CDMA systems is the use of smart antennas. Indeed, detectors equipped with antenna arrays can process signals in both temporal and spatial domains, increase the reliability of the links via diversity, and separate interferers via beamforming. The literature on the combined use of antenna arrays and DF structures is relatively unexplored.

In this paper, we propose a novel space-time MMSE DF detection scheme for uplink DS-CDMA systems with antenna arrays, which employs multiple-parallel-feedback (MPF) branches for interference cancellation. The basic idea is to improve the conventional S-DF structure by using different orders of cancellation and then select the most likely estimate. For each user, the proposed detection structure is equipped

Manuscript received March 23, 2008; revised October 10, 2008, January 14, 2009, and April 3, 2009. First published May 12, 2009; current version published October 2, 2009. This paper was presented in part at the IEEE International Symposium Wireless Communication Systems, Trondheim, Norway, October 16–19, 2007. The review of this paper was coordinated by Prof. H.-C. Wu.

The authors are with the Communications Research Group, Department of Electronics, University of York, YO10 5DD York, U.K. (e-mail: yc521@york.ac.uk; rcdl500@ohm.york.ac.uk).

Color versions of one or more of the figures in this paper are available online at http://ieeexplore.ieee.org.

Digital Object Identifier 10.1109/TVT.2009.2022830

with several parallel branches, which employ different ordering patterns, i.e., each branch produces a symbol estimate by exploiting a certain ordering pattern. Thus, there is a group of symbol estimates at the end of the MPF branch structure. The criterion of the Euclidean distance is used to select the branch with the best performance. The novel structure exploits different patterns and orderings for the modification of the original S-DF architecture and achieves higher detection diversity by selecting the branch that yields the estimates with the best performance. A near-optimal user-ordering algorithm is described for the proposed space-time MPF-DF structure due to the high complexity of the optimal ordering algorithm. Furthermore, the proposed DF receiver structure is combined with cascaded DF stages to mitigate the deleterious effects of error propagation and refine the symbol estimates of the users. We present modified adaptive algorithms for both feedforward and feedback filters using stochastic gradient (SG) and recursive least squares (RLS) algorithms. Basically, we use a switching rule among different ordering branches; for each iteration, we select the optimum branch based on all the feedback results and adapt the filters using the selected branch of data. The performance of the system with beamforming and diversity configurations is also considered. We derive the expressions of the signal-to-interference-plus noise ratio (SINR) for the beamforming and diversity configurations with linear receivers and the expressions of MMSE achieved by the considered DF structures with imperfect and perfect feedback. The main contributions of this paper are given here. 1) Novel space-time MMSE DF receivers with MPF are introduced for interference suppression in uplink DS-CDMA systems with antenna arrays, where beamforming and diversity configurations are considered. 2) The proposed space-time MPF-DF receiver is combined with multistage detection. 3) The modified adaptive algorithms are developed for both feedforward and feedback filters. 4) Analytical works are carried out for the proposed space-time MPF-DF. Our proposed space-time adaptive DF scheme and algorithms can be used in other scenarios, including multiple-input–multiple-output and multicarrier CDMA (MC-CDMA) systems.

This paper is structured as follows: Section II briefly describes the DS-CDMA system model and array configurations. The proposed space-time MPF-DF scheme is described in Section III. Section IV is devoted to the proposed scheme, combined with the cascaded DF stages. The proposed MMSE space-time estimators are derived in Section V, and Section VI discusses the adaptive estimation algorithms for feedforward and feedback receivers. Section VII presents and discusses the simulation results. Section VIII draws the conclusions.

II. DS-CDMA System Model and Array Configurations

Let us consider the uplink of an uncoded synchronous binary phase-shift keying DS-CDMA system with K users, N chips per symbol, and L_p propagation paths. It should be remarked that a synchronous model is assumed for simplicity, although it captures most of the features of more realistic asynchronous models with small-to-moderate delay spreads. The baseband signal transmitted by the kth active user to the base station is given by

$$x_k(t) = A_k \sum_{i=-\infty}^{\infty} b_k(i) s_k(t - iT) \tag{1}$$

where $b_k(i) \in \{\pm 1\}$ denotes the ith symbol for user k, and the real-valued spreading waveform and the amplitude associated with user k are $s_k(t)$ and A_k, respectively. The spreading waveforms are expressed by $s_k(t) = \sum_{i=1}^{N} a_k(i)\phi(t - iT_c)$, where $a_k(i) \in \{\pm 1/\sqrt{N}\}$, $\phi(t)$ is the chip waveform, T_c is the chip duration, and $N = T/T_c$ is the processing gain. Assuming that the channel modeled as parameter vector $\mathbf{h}$ is constant during each symbol and the base station receiver with a J-element linear antenna array is synchronized with the main path, the received signal at the jth antenna element is

$$r_j(t) = \sum_{k=1}^{K} \sum_{l=0}^{L_p - 1} h_{j,k,l}(t) x_k(t - \tau_{j,k,l}) + n_j(t) \tag{2}$$

where $h_{j,k,l}$ and $\tau_{j,k,l}$ are the channel coefficient and the delay associated with the lth path and the kth user of the jth ($j = 1, 2, \ldots, J$) antenna element, respectively. Assuming that delays $\tau_{j,k,l}$ are multiples of the chip rate, the received signal at each antenna $r_j(t)$ after filtering by a chip-pulse matched filter and sampled at the chip rate yields the M-dimensional received vector for each antenna element

$$\begin{aligned} \mathbf{r}_j(i) &= \sum_{k=1}^{K} \left(A_k b_k(i) \mathbf{C}_k \mathbf{h}_{j,k}(i) + \boldsymbol{\eta}_{j,k}(i) \right) + \mathbf{n}_j(i) \\ &= \sum_{k=1}^{K} \left(A_k b_k(i) \widetilde{\mathbf{p}}_{k,j}(i) + \boldsymbol{\eta}_{j,k}(i) \right) + \mathbf{n}_j(i) \end{aligned} \tag{3}$$

where $M = N + L_p - 1$, $\mathbf{n}_j(i) = [n_{j,1}(i), \ldots, n_{j,M}(i)]^T$ is the complex Gaussian noise vector, and $(.)^T$ denotes transpose. The user k channel vector of the jth antenna element is $\mathbf{h}_{j,k}(i) = [h_{j,k,0}(i), \ldots, h_{j,k,L_p-1}(i)]^T$, where $h_{j,k,l}(i) = h_{j,k,l}(iT_c), l = 0, \ldots, L_p - 1$; $\boldsymbol{\eta}_{j,k}(i)$ is the intersymbol interference (ISI) and assumes that the channel order is not greater than N, i.e., $L_p - 1 \leq N$; $\mathbf{s}_k = [a_k(1), \ldots, a_k(N)]^T$ is the signature sequence for user k; and $\widetilde{\mathbf{p}}_{k,j}(i) = \mathbf{C}_k \mathbf{h}_{j,k}(i)$ is the effective signature sequence for user k at the jth antenna element, where the $M \times L_p$ convolution matrix $\mathbf{C}_k$ contains one-chip shifted versions of $\mathbf{s}_k$

$$\mathbf{C}_k = \begin{pmatrix} a_k(1) & & \mathbf{0} \\ \vdots & \ddots & a_k(1) \\ a_k(N) & & \vdots \\ \mathbf{0} & \ddots & a_k(N) \end{pmatrix}.$$

We stack the samples of the received data at each antenna element in a $JM \times 1$ vector so that the coherently demodulated

composite received signal of the antenna-array system is

$$\mathbf{r}(i) = \begin{pmatrix} \mathbf{r}_1(i) \\ \mathbf{r}_2(i) \\ \vdots \\ \mathbf{r}_J(i) \end{pmatrix} = \sum_{k=1}^{K} \widetilde{\mathbf{x}}_k(i) + \mathbf{n}(i) \tag{4}$$

where $\widetilde{\mathbf{x}}_k(i)$ is a JM-dimensional vector and a stack of vectors $A_k b_k(i)\widetilde{\mathbf{p}}_{k,j}(i) + \boldsymbol{\eta}_{j,k}(i)$, $j = 1, \ldots, J$, for user k; $\mathbf{n}(i) = [\mathbf{n}_1^T(i), \ldots, \mathbf{n}_J^T(i)]^T$; and $E[\mathbf{n}(i)\mathbf{n}^H(i)] = \sigma^2 \mathbf{I}_{JM}$, with $\mathbf{I}_{JM}$ denoting a square identity matrix with dimension JM, $(.)^H$ denoting Hermitian transpose, and $E[.]$ standing for the ensemble average. For the diversity configuration, we space the antenna elements over ten times the wavelength, and therefore, the channel coefficients between every two antenna elements are assumed to be independent. In the beamforming case, the spacing between antenna elements is half-wavelength, and the following relation holds for the kth user channel coefficients relevant to antenna elements $j-1$ and j [18]:

$$h_{j,k,l}(i) = h_{j-1,k,l}(i) e^{-j\phi_l} \tag{5}$$

where $h_{j,k,l}$ is the lth path channel coefficient of the jth antenna element regarding user k, $\phi_l = \pi \sin\theta_l$, and θ_l is the direction of arrival (DOA) of the lth path.

For beamforming or diversity configuration, we can design a $JM \times 1$ feedforward filter for each user, which combines the signals from different antennas. Specifically, regarding diversity, to reduce the length of the feedforward filter, we can use a group of $M \times 1$ filters $\boldsymbol{\omega}_{k,j}$, $j = 1, \ldots, J$, which correspond to different antennas to separately handle the received vectors, instead of using a long filter [15], and then combine the output signals from each filter by the maximum ratio combining or equal-gain combining methods. The output signal is

$$z_k(i) = \sum_{j=1}^{J} c_{k,j} \boldsymbol{\omega}_{k,j}^H(i) \mathbf{r}_j(i) \tag{6}$$

where $c_{k,j}$ is the combining weight, and $\mathbf{r}_j(i)$ is the $M \times 1$ received data from antenna element j. In the succeeding parts, we present the novel structure based on the long feedforward filter structure for notation simplicity, even though we remark that, for a diversity configuration, a designer can resort to the approach previously outlined. In the Appendix, we analytically study the beamforming and diversity configurations and draw conclusions on their use.

III. Space-Time MPF DF Receiver Structure

In this section, we present the principles and structures of the proposed space-time MMSE DF detector with MPF branches (MPF-DF) for interference cancellation. The proposed algorithm employs different orders of cancellation to produce a group of estimate candidates, and based on the Euclidean distance, our approach selects the most likely estimate.

The space-time or multiantenna MPF-DF structure is shown in Fig. 1. The proposed receiver employs B parallel branches of successive interference cancellation (SIC) with different orders of feedback for the kth user, where $k = 1, \ldots, K$, with K being the number of users. We equip the βth branch of the kth user with a pair of feedforward and feedback filters, i.e., $JM \times 1$ vector $\mathbf{w}_{\beta,k}(i)$ and $JM \times 1$ vector $\mathbf{f}_{\beta,k}(i)$, where $\beta = 1, \ldots, B$. According to those branches, each user obtains a group of different multiuser interference estimates, which are respectively subtracted from the soft outputs of the feedforward filters. The output of the βth branch for the kth user is

$$z_{\beta,k}(i) = \mathbf{w}_{\beta,k}^H(i)\mathbf{r}(i) - \mathbf{f}_{\beta,k}^H(i)\left[\mathbf{T}_\beta^H \hat{\mathbf{b}}(i)\right] \tag{7}$$

where the $JM \times 1$ received vector $\mathbf{r}(i)$ is the input to a nonlinear structure, and $\hat{\mathbf{b}}(i)$ is the $K \times 1$ feedback vector, i.e., the tentative decision vector of the preceding iteration at time i; in this paper, the DF receiver only employs one iteration, and the value of the feedback vector is computed by $\hat{\mathbf{b}}(i) = \mathrm{sgn}[\Re(\mathbf{W}_{\mathrm{lin}}^H(i)\mathbf{r}(i))]$, where $\mathbf{W}_{\mathrm{lin}}$ is a $JM \times K$ linear filtering matrix designed by the MMSE criterion, and the operator $(.)^H$ denotes Hermitian transpose, $\Re(.)$ selects the real part, and $\mathrm{sgn}(.)$ is the signum function. Matrices $\mathbf{T}_\beta$ are permutated square identity $\mathbf{I}_K$ matrices with dimension K, whose structures for an $B = 4$-branch MPF-DF scheme are given by

$$\mathbf{T}_1 = \mathbf{I}_K, \qquad \mathbf{T}_2 = \begin{pmatrix} \mathbf{0}_{K/4,3K/4} & \mathbf{I}_{3K/4} \\ \mathbf{I}_{K/4} & \mathbf{0}_{K/4,3K/4} \end{pmatrix}$$

$$\mathbf{T}_3 = \begin{pmatrix} \mathbf{0}_{K/2} & \mathbf{I}_{K/2} \\ \mathbf{I}_{K/2} & \mathbf{0}_{K/2} \end{pmatrix}, \quad \mathbf{T}_4 = \begin{pmatrix} 0 & \ldots & 1 \\ \vdots & \ddots & \vdots \\ 1 & \ldots & 0 \end{pmatrix} \tag{8}$$

where $\mathbf{0}_{m,n}$ denotes an $m \times n$-dimensional matrix full of zeros, and the structures of permutation matrices $\mathbf{T}_\beta$ correspond to phase shifts regarding the cancellation order of the users. The purpose of the matrices in (8) is to change the order of cancellation. Specifically, the preceding matrices perform the cancellation with the following order with respect to user powers: $\mathbf{T}_1$ with indices $1, \ldots, K$; $\mathbf{T}_2$ with indices $K/4, K/4+1, \ldots, K, 1, \ldots, K/4-1$; $\mathbf{T}_3$ with indices $K/2, K/2+1, \ldots, K, 1, \ldots, K/2-1$; and $\mathbf{T}_4$ with $K, \ldots, 1$ (reverse order). Quantity $\mathbf{T}_\beta^H \hat{\mathbf{b}}(i)$ is the feedback vector corresponding to the βth branch. For more branches, additional phase shifts are applied with respect to user cancellation ordering. Note that different update orders were tested, although they did not result in performance improvement.

The feedback filter $\mathbf{f}_{\beta,k}(i)$ controls the permutated feedback vector $\mathbf{T}_\beta^H \hat{\mathbf{b}}(i)$. The structure of the feedback filter is given by $\mathbf{f}_{\beta,k}(i) = [f_{\beta,k,1}(i), f_{\beta,k,2}(i), \ldots, f_{\beta,k,K}(i)]^T$, where elements $f_{\beta,k,\gamma}(i) = 0$ (when $k \le \gamma \le K$, $\gamma = 1, \ldots, K$), and operator $(.)^T$ denotes transpose. The nonzero elements of the filter $\mathbf{f}_{\beta,k}(i)$ correspond to the number of used feedback connections and the users to be canceled.

The number of parallel branches B that yield detection candidates is a parameter that must be chosen by the designer. The number of candidates of the optimal ordering algorithm is $B = K!$ and is clearly very complex for practical systems. The goal of the proposed scheme is to improve performance using parallel searches and to select the most likely symbol estimate.

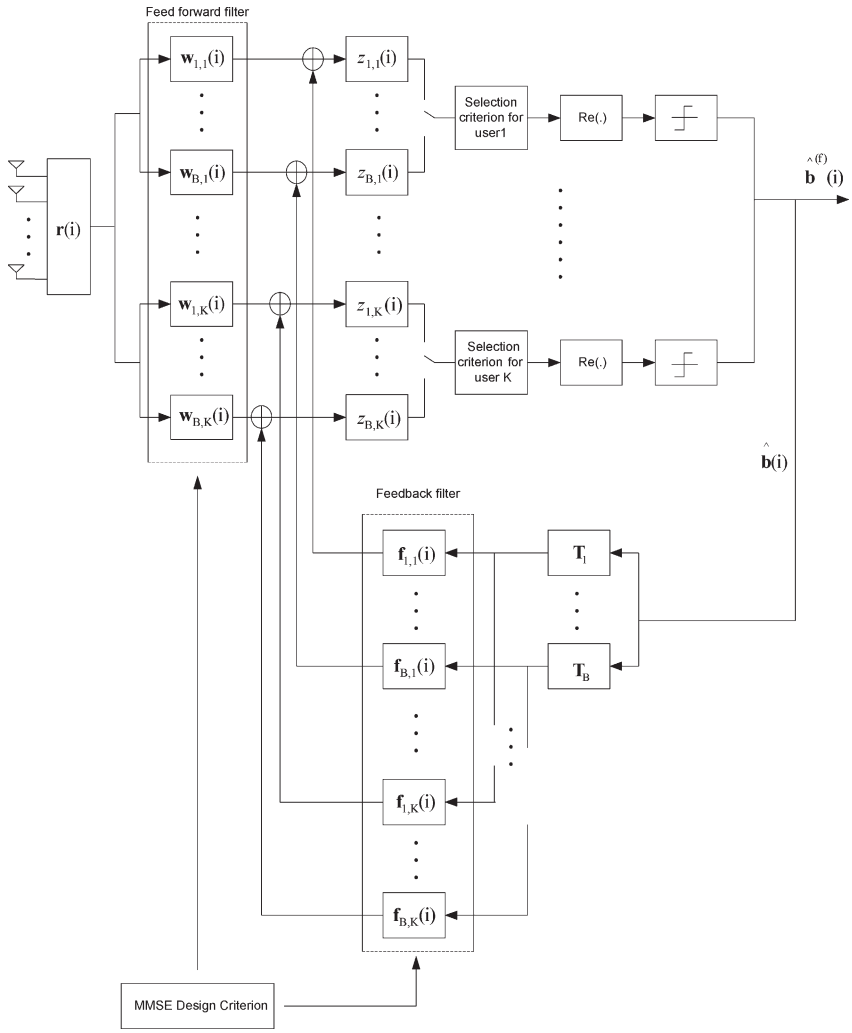

Fig. 1. Proposed multiantenna MPF-DF receiver structure.

The final output $\hat{b}_k^{(f)}(i)$ for the kth user of the space-time MPF-DF detector chooses the best estimate of the B candidates based on the criterion of the Euclidean distance for each symbol interval i, as described by

$$\beta_{\mathrm{opt},k} = \arg \min_{\beta \in \{1,\ldots,B\}} e_{\beta,k}(i) \tag{9}$$

$$\hat{b}_k^{(f)}(i) = \mathrm{sgn}\left[\Re\left(z_{\beta_{\mathrm{opt},k}}(i)\right)\right] \tag{10}$$

where $e_{\beta,k}(i) = |b_k(i) - z_{\beta,k}(i)|$, and $\hat{b}_k^{(f)}(i)$ forms the vector of final decisions $\hat{\mathbf{b}}_k^{(f)}(i) = [\hat{b}_1^{(f)}(i), \ldots, \hat{b}_K^{(f)}(i)]^T$. Our studies indicate that the $B = 4$ near-optimal user-ordering algorithm achieves most of the gains of the proposed structure and offers a good tradeoff between performance and complexity.

IV. Multistage Space-Time MPF-DF Detection

In this section, the proposed receiver structure is considered in conjunction with cascaded DF stages [9], [10], which are of great interest for uplink scenarios due to the capability of providing uniform performance over the users.

In [9], Woodward *et al.* presented a multistage detector with an S-DF in the first stage and P-DF or S-DF structures, with the users being demodulated in reverse order in the second stage. First, let us describe the multistage receiver with only the S-DF or the P-DF detector; for the first stage $m = 1$, we have the output defined by

$$\hat{\mathbf{b}}^{(m-1)}(i) = \mathrm{sgn}\left[\Re\left(\mathbf{W}_{\mathrm{lin}}^H(i)\mathbf{r}(i)\right)\right] \tag{11}$$

$$\mathbf{z}^{(m)}(i) = \mathbf{W}^{(m)H}(i)\mathbf{r}(i) - \mathbf{F}^{(m)H}(i)\hat{\mathbf{b}}^{(m-1)}(i). \tag{12}$$

For stages $m \geq 2$, we obtain

$$\hat{\mathbf{b}}^{(m-1)}(i) = \mathrm{sgn}\left[\Re\left(\mathbf{z}^{(m-1)}(i)\right)\right] \tag{13}$$

$$\mathbf{z}^{(m)}(i) = \left[\mathbf{W}^{(m)}(i)\mathbf{M}\right]^H \mathbf{r}(i) - \left[\mathbf{M}\mathbf{F}^{(m)}(i)\right]^H \hat{\mathbf{b}}^{(m-1)}(i) \tag{14}$$

where the number of stages m depends on the application. More stages can be added; the order of the users is reversed from stage to stage; the $JM \times K$ filtering matrix $\mathbf{W}^{(m)}$ is given by $\mathbf{W}^{(m)}(i) = [\mathbf{w}_1^{(m)}(i), \ldots, \mathbf{w}_K^{(m)}(i)]$; the $K \times K$ matrix $\mathbf{F}^{(m)}$ is given by $\mathbf{F}^{(m)}(i) = [\mathbf{f}_1^{(m)}(i), \ldots, \mathbf{f}_K^{(m)}(i)]$, where $\mathbf{w}_k^{(m)}(i)$ and $\mathbf{f}_k^{(m)}(i)$ are the $JM \times 1$ and $K \times 1$ filtering vectors corresponding to the kth user $k = 1, \ldots, K$; $\hat{\mathbf{b}}^{(m-1)}(i)$ is the

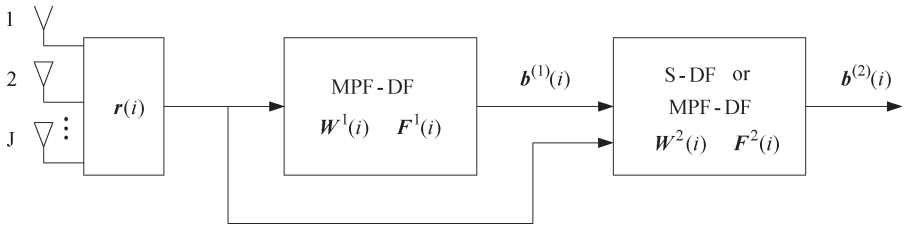

Fig. 2. Two-stage DF receiver with space-time MPF-DF scheme in the first stage.

$K \times 1$ vector of the $(m-1)$th stage tentative decisions; and $\mathbf{M}$ is a $K \times K$ square permutation matrix with ones along the reverse diagonal and zeros elsewhere [similar to $\mathbf{T}_4$ in (8)]. The $K \times 1$ decision vector of the mth stage $\mathbf{z}^{(m)}(i) = [z_1^{(m)}(i), \ldots, z_K^{(m)}(i)]^T$.

Let us now focus on the proposed algorithm and combine the space-time MPF-DF structure with multistage detection. To equalize the performance over the user population, we consider a two-stage structure, i.e., $m = 2$, as shown in Fig. 2. The first stage is an MPF-DF scheme. To evaluate the performance of the proposed multistage schemes, an S-DF and an MPF-DF are considered in the second stage. The multistage receiver system is denoted as IMPFS-DF when an S-DF is employed in the second stage. The output of the second stage of the IMPFS-DF scheme is shown in (14). Note that feedback vector $\hat{\mathbf{b}}^{(1)}(i)$ is the output of an MPF-DF receiver, which is introduced in Section III. The proposed multistage scheme is denoted as IMPFMPF-DF and corresponds to an MPF-DF architecture employed in both stages. The jth component of the soft output vector $\mathbf{z}_\beta^{(2)}(i)$ corresponding to the βth branch of its second stage is

$$z_{\beta,j}^{(2)}(i) = \left[\mathbf{W}_\beta^{(2)}(i)\mathbf{M}\right]_j^H \mathbf{r}(i) - \left[\mathbf{T}_\beta \mathbf{F}_\beta^{(2)}(i)\right]_j^H \hat{\mathbf{b}}^{(1)}(i) \quad (15)$$

where $[.]_j$ denotes the jth column of the argument (a matrix), and the second-stage MPF-DF filtering matrices corresponding to the βth branch are given by $\mathbf{W}_\beta^{(2)}(i) = [\mathbf{w}_{\beta,1}^{(2)}(i), \ldots, \mathbf{w}_{\beta,K}^{(2)}(i)]$ and $\mathbf{F}_\beta^{(2)}(i) = [\mathbf{f}_{\beta,1}^{(2)}(i), \ldots, \mathbf{f}_{\beta,K}^{(2)}(i)]$, where $\mathbf{w}_{\beta,k}^{(2)}(i)$ and $\mathbf{f}_{\beta,k}^{(2)}(i)$ are the $JM \times 1$ and $K \times 1$ filtering vectors corresponding to the βth branch of the kth $(k = 1, \ldots, K)$ user. The final decision is

$$\beta_{\mathrm{opt},j} = \arg \min_{\beta \in \{1,\ldots,B\}} e_{\beta,j}^{(2)}(i) \quad (16)$$

$$\hat{b}_j^{(2)}(i) = \mathrm{sgn}\left[\Re\left(z_{\beta_{\mathrm{opt},j}}^{(2)}(i)\right)\right] \quad (17)$$

where $e_{\beta,j}^{(2)}(i) = |b_k(i) - z_{\beta,j}^{(2)}(i)|$. The role of reversing the cancellation order in successive stages is to equalize the performance of the users over the population or at least reduce the performance disparities.

V. MMSE Design of the Proposed Space-Time Estimators

Let us describe in this section the design of the proposed space-time MMSE DF detectors. A general case where each branch has a pair of feedforward and feedback filters is considered. First, let us consider the cost function for branch β of user k, i.e.,

$$\begin{aligned} J_{\mathrm{MSE}} &= E\left[\left|b_k(i) - \mathbf{w}_{\beta,k}^H(i)\mathbf{r}(i) + \mathbf{f}_{\beta,k}^H(i)\hat{\mathbf{b}}_\beta(i)\right|^2\right] \\ &= \sigma_b^2 - \mathbf{w}_{\beta,k}^H(i)\mathbf{p}_k - \mathbf{p}_k^H\mathbf{w}_{\beta,k}(i) + \mathbf{w}_{\beta,k}^H(i)\mathbf{R}\mathbf{w}_{\beta,k}(i) \\ &\quad + \mathbf{f}_{\beta,k}^H(i)E\left[\hat{\mathbf{b}}_\beta(i)\hat{\mathbf{b}}_\beta^H(i)\right]\mathbf{f}_{\beta,k}(i) \\ &\quad - \mathbf{w}_{\beta,k}^H(i)\mathbf{B}\mathbf{f}_{\beta,k}(i) - \mathbf{f}_{\beta,k}^H(i)\mathbf{B}^H\mathbf{w}_{\beta,k}(i) \end{aligned} \quad (18)$$

where $\hat{\mathbf{b}}_\beta(i) = \mathbf{T}_\beta^H\hat{\mathbf{b}}(i)$ is the feedback vector of branch β; $\mathbf{T}_\beta$ is the permutation matrix, which is used to change the order of cancellation; and $\mathbf{w}_{\beta,k}(i)$ and $\mathbf{f}_{\beta,k}(i)$ have been described in Section III. The associated covariance matrices are $\mathbf{R} = E[\mathbf{r}(i)\mathbf{r}^H(i)] = \mathbf{P}\mathbf{P}^H + \sigma^2\mathbf{I}$, $\sigma_b^2 = E[|b_k(i)|^2]$, and $\mathbf{B} = E[\mathbf{r}(i)\hat{\mathbf{b}}_\beta^H(i)]$. Here, we define the matrices of effective spreading sequences $\mathbf{P} = [\mathbf{p}_1, \ldots, \mathbf{p}_K]$, $\mathbf{p}_k = [\widetilde{\mathbf{p}}_{k,1}^T, \ldots, \widetilde{\mathbf{p}}_{k,J}^T]^T$, and $\widetilde{\mathbf{p}}_{k,j} = \mathbf{C}_k\mathbf{h}_{j,k}(i)$, which is the $M \times 1$ effective spreading sequence of user k $(k = 1, \ldots, K)$ regarding the jth $(j = 1, \ldots, J)$ antenna. To minimize the cost function in (18), we first take the gradient with respect to filter $\mathbf{w}_{\beta,k}(i)$ and $\mathbf{f}_{\beta,k}(i)$, which yields

$$\bigtriangledown J_{\mathbf{w}_{\beta,k}^*(i)} = \mathbf{R}\mathbf{w}_{\beta,k}(i) - \mathbf{p}_k - \mathbf{B}\mathbf{f}_{\beta,k}(i) \quad (19)$$

$$\bigtriangledown J_{\mathbf{f}_{\beta,k}^*(i)} = \left(E\left[\hat{\mathbf{b}}_\beta(i)\hat{\mathbf{b}}_\beta^H(i)\right]\right)\mathbf{f}_{\beta,k}(i) - \mathbf{B}^H\mathbf{w}_{\beta,k}(i). \quad (20)$$

Thus, the solution can be obtained by setting the gradient terms equal to zero, i.e.,

$$\mathbf{w}_{\beta,k}(i) = \mathbf{R}^{-1}\left(\mathbf{p}_k + \mathbf{B}\mathbf{f}_{\beta,k}(i)\right) \quad (21)$$

$$\begin{aligned} \mathbf{f}_{\beta,k}(i) &= \left(E\left[\hat{\mathbf{b}}_\beta(i)\hat{\mathbf{b}}_\beta^H(i)\right]\right)^{-1}\mathbf{B}^H\mathbf{w}_{\beta,k}(i) \\ &\approx \mathbf{B}^H\mathbf{w}_{\beta,k}(i). \end{aligned} \quad (22)$$

If we assume imperfect feedback, then $E[\hat{\mathbf{b}}_\beta(i)\hat{\mathbf{b}}_\beta^H(i)] = E[\mathbf{T}_\beta^H\hat{\mathbf{b}}(i)\hat{\mathbf{b}}^H(i)\mathbf{T}_\beta] \approx \mathbf{I}_K$ for small error rates. The complexities of (21) and (22) are $O((JM)^3)$ and $O(K^3)$ due to the matrix inversion.

In the Appendix, we mathematically study the associated MMSE for the general space-time DF receivers (S-DF and P-DF with antenna arrays) and the proposed space-time MPF-DF scheme with imperfect and perfect feedback.

VI. Adaptive Estimation Algorithms

In this section, we present modified SG and RLS algorithms to estimate the feedforward and feedback filters of the proposed multiantenna MPF-DF receiver using MMSE criteria. To

reduce the complexity, we consider employing one-feedforward and one-feedback adaptive filters for all B branches, instead of multiple-feedforward and multiple-feedback filters. Note that multiple filters have been considered in our studies; however, they did not yield better results than the single-filter approach adopted here. We show these results in the simulation section. In the proposed algorithms, for each iteration, we select the optimum branch based on all the feedback results and adapt the filters using the branch of data with the lowest metric.

A. SG Algorithm

Let us first discuss SG algorithms and then consider the cost function based on the mean squared error (MSE) criterion

$$J_{\mathrm{MSE}} = E\left[\left|b_k(i) - \mathbf{w}_k^H(i)\mathbf{r}(i) + [\mathbf{T}_\beta \mathbf{f}_k(i)]^H \hat{\mathbf{b}}(i)\right|^2\right] \quad (23)$$

where $\mathbf{T}_\beta$ are the permutation matrices, which are employed to change the cancellation order of the users. For each iteration, we select the most likely branch before adapting $\mathbf{w}_k(i)$ and $\mathbf{f}_k(i)$

$$\beta_{\mathrm{opt},k} = \arg \min_{\beta\in\{1,\ldots,B\}} e_{\beta,k}(i) \quad (24)$$

$$e_{\beta,k}(i) = |b_k(i) - z_{\beta,k}(i)|. \quad (25)$$

The best branch $\beta_{\mathrm{opt},k}$ is selected to minimize the Euclidean distance. The final output $\hat{\mathbf{b}}_k^{(f)}(i)$ chooses the best estimate from the B candidates for each symbol interval i. The SG solution to (23) can be devised by using instantaneous estimates and taking the gradient terms with respect to $\mathbf{w}_k^*(i)$ and $\mathbf{f}_k(i)^*$, which should adaptively minimize J_{MSE}. Using the selected branch $\beta_{\mathrm{opt},k}$, we obtain the expressions of the SG as

$$\begin{aligned}\bigtriangledown J_{\mathbf{w}_k^*(i)} = &-\Big(b_k^*(i) - \mathbf{r}^H(i)\mathbf{w}_k(i) \\ &+ \hat{\mathbf{b}}^H(i)\mathbf{T}_{\beta_{\mathrm{opt},k}}\mathbf{f}_k(i)\Big)\mathbf{r}(i) \quad (26)\end{aligned}$$

$$\begin{aligned}\bigtriangledown J_{\mathbf{f}_k^*(i)} = &\Big(b_k^*(i) - \mathbf{r}^H(i)\mathbf{w}_k(i) \\ &+ \hat{\mathbf{b}}^H(i)\mathbf{T}_{\beta_{\mathrm{opt},k}}\mathbf{f}_k(i)\Big)\mathbf{T}^H_{\beta_{\mathrm{opt},k}}\hat{\mathbf{b}}(i). \quad (27)\end{aligned}$$

According to the SG or LMS filter theory in [17], we have the following update equations:

$$\mathbf{w}_k(i+1) = \mathbf{w}_k(i) - \mu_{\mathbf{w}} \bigtriangledown J_{\mathbf{w}_k^*(i)} \quad (28)$$

$$\mathbf{f}_k(i+1) = \mathbf{f}_k(i) - \mu_{\mathbf{f}} \bigtriangledown J_{\mathbf{f}_k^*(i)} \quad (29)$$

where $\mu_{\mathbf{w}}$ and $\mu_{\mathbf{f}}$ are the values of the step size. Substituting (26) and (27) into (28) and (29), respectively, we arrive at the update equations for the estimation of $\mathbf{w}_k(i)$ and $\mathbf{f}_k(i)$ based on the SG algorithms

$$\mathbf{w}_k(i+1) = \mathbf{w}_k(i) + \mu_{\mathbf{w}}\epsilon^*(i)\mathbf{r}(i) \quad (30)$$

$$\mathbf{f}_k(i+1) = \mathbf{f}_k(i) - \mu_{\mathbf{f}}\epsilon^*(i)\mathbf{T}^H_{\beta_{\mathrm{opt},k}}\hat{\mathbf{b}}(i) \quad (31)$$

where $\epsilon(i) = b_k(i) - (\mathbf{w}_k^H(i)\mathbf{r}(i) - \mathbf{f}_k^H(i)\mathbf{T}^H_{\beta_{\mathrm{opt},k}}\hat{\mathbf{b}}(i))$. The steps of the algorithm are summarized in Table I. Due to the fact that most elements of the permutation matrices are zeros, our SG algorithm can be implemented with linear complexity.

TABLE I
PROPOSED ADAPTIVE ESTIMATION ALGORITHM: SG

Step 1:	Choose intial values for $\mathbf{w}_k$ and $\mathbf{f}_k$, and appropriate step sizes $\mu_{\mathbf{w}}$, $\mu_{\mathbf{f}}$.	
Step 2:	For i=0, 1, 2, ...	
	(1)	compute the feedback vectors $\mathbf{T}_\beta^H\hat{\mathbf{b}}(i)$ and the outputs for different branches of the proposed space-time MPF-DF detector
	(2)	select the most likely branch $\beta_{opt,k} = \arg\min_{\beta\in\{1,\ldots,B\}} e_{\beta,k}(i)$
	(3)	update $\mathbf{w}_k(i+1) = \mathbf{w}_k(i) + \mu_{\mathbf{w}}\epsilon^*(i)\mathbf{r}(i)$
	(4)	update $\mathbf{f}_k(i+1) = \mathbf{f}_k(i) - \mu_{\mathbf{f}}\epsilon^*(i)\mathbf{T}^H_{\beta_{opt,k}}\hat{\mathbf{b}}(i)$

It is worth noting that, for stability and to facilitate tuning of parameters, it is useful to employ normalized step sizes when operating in a changing environment. The normalized version of this algorithm is described by $\mu'_{\mathbf{w}} = \mu_{\mathbf{w}}/(\mathbf{r}^H(i)\mathbf{r}(i))$ and $\mu'_{\mathbf{f}} = \mu_{\mathbf{f}}/(\hat{\mathbf{b}}^H(i)\mathbf{T}_{\beta_{\mathrm{opt},k}}\mathbf{T}^H_{\beta_{\mathrm{opt},k}}\hat{\mathbf{b}}(i))$.

B. RLS Algorithm

Let us consider the RLS algorithm for feedforward and feedback filters. According to the RLS theory in [17], we express the cost function to be minimized as $\xi(i)$, where i is the length of the observable data. In addition, it is customary to introduce a forgetting factor λ into the definition of cost function $\xi(i)$. We thus write

$$\xi(i) = \sum_{n=1}^{i} \lambda^{i-n}\left|b_k(n) - \mathbf{w}_k^H(i)\mathbf{r}(n) + [\mathbf{T}_\beta\mathbf{f}_k(i)]^H\hat{\mathbf{b}}(n)\right|^2. \quad (32)$$

For each iteration, we select the most likely branch corresponding to the minimum Euclidean distance

$$\beta_{\mathrm{opt},k} = \arg \min_{\beta\in\{1,\ldots,B\}} e_{\beta,k}(i) \quad (33)$$

$$e_{\beta,k}(i) = |b_k(i) - z_{\beta,k}(i)|. \quad (34)$$

The RLS solution to (32) can be obtained by taking the gradient of (32) with respect to $\mathbf{w}_k^*(i)$. Using the selected branch $\beta_{\mathrm{opt},k}$ yields

$$\begin{aligned}\bigtriangledown\xi_{\mathbf{w}_k^*(i)} = &-\sum_{n=1}^{i}\lambda_{\mathbf{w}}^{i-n}\mathbf{r}(n)b_k(n) + \sum_{n=1}^{i}\lambda_{\mathbf{w}}^{i-n}\mathbf{r}(n)\mathbf{r}^H(n)\mathbf{w}_k(i) \\ &- \sum_{n=1}^{i}\lambda_{\mathbf{w}}^{i-n}\mathbf{r}(n)\hat{\mathbf{b}}^H(n)\mathbf{T}_{\beta_{\mathrm{opt},k}}\mathbf{f}_k(i). \quad (35)\end{aligned}$$

Let us further define

$$\mathbf{a}_k(i) = -\sum_{n=1}^{i}\lambda_{\mathbf{w}}^{i-n}\mathbf{r}(n)b_k(n) \quad (36)$$

$$\mathbf{R}(i) = \sum_{n=1}^{i}\lambda_{\mathbf{w}}^{i-n}\mathbf{r}(n)\mathbf{r}^H(n) \quad (37)$$

$$\mathbf{B}_k(i) = \sum_{n=1}^{i}\lambda_{\mathbf{w}}^{i-n}\mathbf{r}(n)\hat{\mathbf{b}}^H(n)\mathbf{T}_{\beta_{\mathrm{opt},k}}. \quad (38)$$

Then, by setting $\bigtriangledown\xi_{\mathbf{w}_k^*(i)} = 0$, we obtain

$$\mathbf{w}_k(i) = \mathbf{R}^{-1}(i)\left[\mathbf{B}_k(i)\mathbf{f}_k(i) + \mathbf{a}_k(i)\right]. \quad (39)$$

Because $\mathbf{R}(i) = \lambda_{\mathbf{w}}\mathbf{R}(i-1) + \mathbf{r}(i)\mathbf{r}^H(i)$ and based on the matrix inversion lemma in [17], the update equation for $\mathbf{R}^{-1}(i)$ is given by

$$\mathbf{R}^{-1}(i) = \lambda_{\mathbf{w}}^{-1}\mathbf{R}^{-1}(i-1) - \lambda_{\mathbf{w}}^{-1}\mathbf{q}_1(i)\mathbf{r}^H(i)\mathbf{R}^{-1}(i-1) \tag{40}$$

where $\mathbf{q}_1(i) = \mathbf{u}_1(i)/(\lambda_{\mathbf{w}} + \mathbf{r}^H(i)\mathbf{u}_1(i))$, and $\mathbf{u}_1(i) = \mathbf{R}^{-1}(i-1)\mathbf{r}(i)$. We also have the following two equations:

$$\mathbf{a}_k(i) = \lambda_{\mathbf{w}}\mathbf{a}_k(i-1) + \mathbf{r}(i)b_k(i) \tag{41}$$

$$\mathbf{B}_k(i) = \lambda_{\mathbf{w}}\mathbf{B}_k(i-1) + \mathbf{r}(i)\hat{\mathbf{b}}^H(i)\mathbf{T}_{\beta_{\mathrm{opt},k}}. \tag{42}$$

By combining (39)–(42), we obtain the RLS algorithm to update feedforward filter $\mathbf{w}_k(i)$.

Following a similar approach to take the gradient of (32) with respect to $\mathbf{f}_k^*(i)$ yields

$$\begin{aligned}\bigtriangledown \xi_{\mathbf{f}_k^*(i)} = &\sum_{n=1}^{i}\lambda_{\mathbf{f}}^{i-n}\mathbf{T}_{\beta_{\mathrm{opt},k}}^H\hat{\mathbf{b}}(n)b_k(n)\\ &-\sum_{n=1}^{i}\lambda_{\mathbf{f}}^{i-n}\mathbf{T}_{\beta_{\mathrm{opt},k}}^H\hat{\mathbf{b}}(n)\mathbf{r}^H(n)\mathbf{w}_k(i)\\ &+\sum_{n=1}^{i}\lambda_{\mathbf{f}}^{i-n}\mathbf{T}_{\beta_{\mathrm{opt},k}}^H\hat{\mathbf{b}}(n)\hat{\mathbf{b}}^H(n)\mathbf{T}_{\beta_{\mathrm{opt},k}}\mathbf{f}_k(i).\end{aligned} \tag{43}$$

Let us define

$$\mathbf{c}_k(i) = \sum_{n=1}^{i}\lambda_{\mathbf{f}}^{i-n}\mathbf{T}_{\beta_{\mathrm{opt},k}}^H\hat{\mathbf{b}}(n)b_k(n) \tag{44}$$

$$\mathbf{D}_k(i) = \sum_{n=1}^{i}\lambda_{\mathbf{f}}^{i-n}\mathbf{T}_{\beta_{\mathrm{opt},k}}^H\hat{\mathbf{b}}(n)\mathbf{r}^H(n) \tag{45}$$

$$\mathbf{S}_k(i) = \sum_{n=1}^{i}\lambda_{\mathbf{f}}^{i-n}\mathbf{T}_{\beta_{\mathrm{opt},k}}^H\hat{\mathbf{b}}(n)\hat{\mathbf{b}}^H(n)\mathbf{T}_{\beta_{\mathrm{opt},k}}. \tag{46}$$

By setting $\bigtriangledown\xi_{\mathbf{f}_k^*(i)} = 0$, we have

$$\mathbf{f}_k(i) = \mathbf{S}_k^{-1}(i)\left[\mathbf{D}_k(i)\mathbf{w}_k(i) - \mathbf{c}_k(i)\right] \tag{47}$$

as well as the following equations:

$$\mathbf{c}_k(i) = \lambda_{\mathbf{f}}\mathbf{c}_k(i-1) + \mathbf{T}_{\beta_{\mathrm{opt},k}}^H\hat{\mathbf{b}}(i)b_k(i) \tag{48}$$

$$\mathbf{D}_k(i) = \lambda_{\mathbf{f}}\mathbf{D}_k(i-1) + \mathbf{T}_{\beta_{\mathrm{opt},k}}^H\hat{\mathbf{b}}(i)\mathbf{r}^H(i). \tag{49}$$

Since $\mathbf{S}_k(i) = \lambda_{\mathbf{f}}\mathbf{S}_k(i-1) + \mathbf{T}_{\beta_{\mathrm{opt},k}}^H\hat{\mathbf{b}}(i)\hat{\mathbf{b}}^H(i)\mathbf{T}_{\beta_{\mathrm{opt},k}}$ and by using the matrix inversion lemma [17], we obtain the update equation for $\mathbf{S}_k^{-1}(i)$, which is given by

$$\mathbf{S}_k^{-1}(i) = \lambda_{\mathbf{f}}^{-1}\mathbf{S}_k^{-1}(i-1) - \lambda_{\mathbf{f}}^{-1}\mathbf{q}_2(i)\hat{\mathbf{b}}^H(i)\mathbf{T}_{\beta_{\mathrm{opt},k}}\mathbf{S}_k^{-1}(i-1) \tag{50}$$

where $\mathbf{q}_2(i) = \mathbf{u}_2(i)/(\lambda_{\mathbf{f}} + \hat{\mathbf{b}}^H(i)\mathbf{T}_{\beta_{\mathrm{opt},k}}\mathbf{u}_2(i))$, and $\mathbf{u}_2(i) = \mathbf{S}_k^{-1}(i-1)\mathbf{T}_{\beta_{\mathrm{opt},k}}^H\hat{\mathbf{b}}(i)$. By combining (47)–(50), we obtain the RLS algorithm for the feedback filter $\mathbf{f}_k(i)$. The steps of the RLS algorithms are summarized in Table II.

TABLE II
PROPOSED ADAPTIVE ESTIMATION ALGORITHM: RLS

Step 1:	Choose intial values for $\mathbf{a}_k$, $\mathbf{B}_k$, $\mathbf{R}_k^{-1}$, $\mathbf{c}_k$, $\mathbf{D}_k$ and $\mathbf{S}_k^{-1}$, and appropriate forgetting factors $\lambda_{\mathbf{w}}$, $\lambda_{\mathbf{f}}$.	
Step 2:	For i=0, 1, 2, ...	
	(1)	compute the feedback vectors $\mathbf{T}_{\beta}^H\hat{\mathbf{b}}(i)$ and the outputs for different branches of the proposed space-time MPF-DF detector
	(2)	select the most likely branch $\beta_{opt,k} = \arg\min_{\beta\in\{1,\ldots,B\}} e_{\beta,k}(i)$
	(3)	update $\mathbf{a}_k(i) = \lambda_{\mathbf{w}}\mathbf{a}_k(i-1) + \mathbf{r}(i)b_k(i)$
	(4)	update $\mathbf{B}_k(i) = \lambda_{\mathbf{w}}\mathbf{B}_k(i-1) + \mathbf{r}(i)\hat{\mathbf{b}}^H(i)\mathbf{T}_{\beta_{opt,k}}$
	(5)	$\mathbf{R}^{-1}(i) = \lambda_{\mathbf{w}}^{-1}\mathbf{R}^{-1}(i-1) - \lambda_{\mathbf{w}}^{-1}\mathbf{q}_1(i)\mathbf{r}^H(i)\mathbf{R}^{-1}(i-1)$
	(6)	update $\mathbf{w}_k(i) = \mathbf{R}^{-1}(i)[\mathbf{B}_k(i)\mathbf{f}_k(i) + \mathbf{a}_k(i)]$
	(7)	update $\mathbf{c}_k(i) = \lambda_{\mathbf{f}}\mathbf{c}_k(i-1) + \mathbf{T}_{\beta_{opt,k}}^H\hat{\mathbf{b}}(i)b_k(i)$
	(8)	update $\mathbf{D}_k(i) = \lambda_{\mathbf{f}}\mathbf{D}_k(i-1) + \mathbf{T}_{\beta_{opt,k}}^H\hat{\mathbf{b}}(i)\mathbf{r}^H(i)$
	(9)	$\mathbf{S}_k^{-1}(i) = \lambda_{\mathbf{f}}^{-1}(\mathbf{S}_k^{-1}(i-1) - \mathbf{q}_2(i)\hat{\mathbf{b}}^H(i)\mathbf{T}_{\beta_{opt,k}}\mathbf{S}_k^{-1}(i-1))$
	(10)	update $\mathbf{f}_k(i) = \mathbf{S}_k^{-1}(i)[\mathbf{D}_k(i)\mathbf{w}_k(i) - \mathbf{c}_k(i)]$

The superior performance of the RLS algorithm compared with that of the SG algorithm is attained at the expense of a large increase in computational complexity. The complexity is evaluated by the number of multiplications. The RLS algorithm requires a total of $O((JM)^2) + O(K^2)$ multiplications, which increase as the square of JM and K, where J is the number of antenna elements, M is the gain of the effective spreading sequence, and K is the number of users. On the other hand, the SG algorithm requires $O(JM) + O(K)$ multiplications, linearly increasing with JM and K. Note, however, that the operations required to compute $\mathbf{R}^{-1}(i)$ are common to all K users and can be used for saving computations.

VII. SIMULATION

In this section, we evaluate the performance of the novel space-time MPF-DF schemes and compare them with other existing structures. We adopt a simulation approach and conduct several experiments to verify the effectiveness of the proposed techniques. We carried out simulations to assess the bit error rate (BER) performance of the DF receivers for different loads, channel fading rates, number of antenna elements, and signal-to-noise ratios. The users in the system are assumed to have a power distribution given by lognormal random variables with an associated standard deviation of 0.5. Our simulation results are based on an uncoded system, and the receivers have access to pilot channels for estimating the filters. We calculate the average BER by taking the average performance over the users. All channels have a profile with three paths, whose powers are $p_0 = 0$ dB, $p_1 = -7$ dB, and $p_2 = -10$ dB, which are normalized. The sequence of channel coefficients $h_l(i) = p_l\psi_l(i)$ $(l = 0, 1, 2)$, where $\psi_l(i)$ is computed according to Jakes' model. We optimized the parameters of the normalized-step-size SG algorithms with step sizes $\mu_{\mathbf{w}} = 0.1$ and $\mu_{\mathbf{f}} = 0.1$ and those of the RLS algorithms with forgetting factors $\lambda_{\mathbf{w}} = 0.998$ and $\lambda_{\mathbf{f}} = 0.998$. We consider packets with 1000 symbols. The DOAs are uniformly distributed in $(0, 2\pi)$. The receiver structure (linear or DF), type of DF scheme, and multiantenna configurations are indicated as follows:

1) S-DF: the S-DF detector in [12] and [13];
2) P-DF: the P-DF detector in [9];

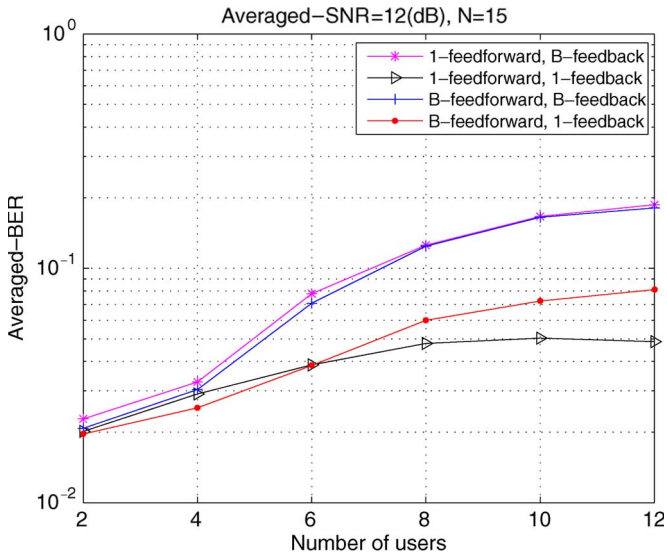

Fig. 3. Four adaptive schemes for the MPF-DF structure.

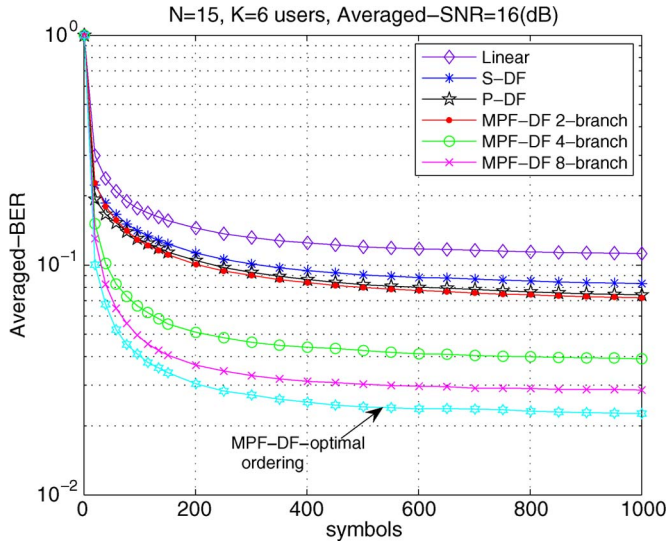

Fig. 4. BER performance versus the number of symbols for normalized SG algorithms, $N = 15$, $K = 6$ users, $f_dT = 5 \times 10^{-5}$, and one-antenna configuration.

3) MPF-DF: the proposed MPF branch DF detector;
4) ISS-DF: the iterative system of Woodward *et al.* [9] with S-DF in the first and second stages;
5) IMPFS-DF: the proposed iterative detector with the novel MPF-DF in the first stage and the S-DF in the second stage;
6) IMPFMPF-DF: the proposed iterative receiver with the MPF-DF in the first and second stages;
7) (D): antenna-array system using the diversity configuration;
8) (B): antenna-array system using the beamforming configuration.

Initially, we study the performance of four different adaptive structures of the proposed MPF-DF, i.e., the multiple-feedforward–multiple-feedback, the multiple-feedforward–single-feedback, the single-feedforward–multiple-feedback, and the single-feedforward–single-feedback structure. Fig. 3 shows the performance of the averaged BER versus the number of users over the four different adaptive schemes in the uplink DS-CDMA system with $N = 15$ Gold sequences. We can see that the single-feedforward and single-feedback adaptive receiver is the best choice since it can support more users than the other structures and has the lowest complexity. In our studies, this was verified for a wide range of scenarios.

In the second experiment, we study the impact of the number of branches on the MPF-DF performance. The DS-CDMA system employs Gold sequences with $N = 15$ as the spreading codes. The normalized-step-size SG algorithms are employed to update feedforward and feedback filters. We designed the novel DF receivers with $B = 2, 4,$ and 8 parallel branches and compared their BER performance versus the number of symbols with the existing S-DF and P-DF structures, as shown in Fig. 4. The results show that the low-complexity ordering algorithm achieves a performance close to that of the optimal ordering while keeping the complexity reasonably low for practical utilization. Furthermore, the performance of the new MPF-DF scheme with $B = 2, 4,$ and 8 outperforms the S-DF and the P-DF detector. It can be noted from the curves that the performance of the new MPF-DF improves as the number of parallel branches increases. In this regard, we also notice that the gains of performance obtained through additional branches decrease as B is increased. Thus, we adopt $B = 4$ for the remaining experiments, because it presents a very attractive tradeoff between performance and complexity. The fading rate is $(f_dT = 5 \times 10^{-5})$ in this experiment.

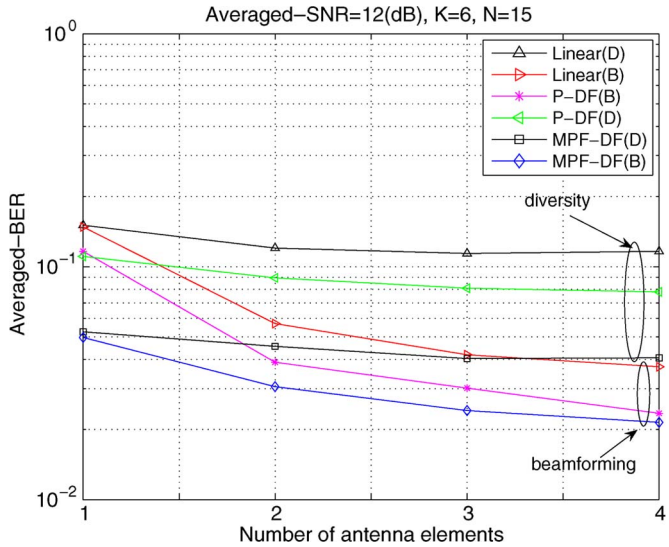

Fig. 5. BER performance versus the number of antennas for normalized SG algorithms, $N = 15$, $K = 6$ users, and $f_dT = 1 \times 10^{-3}$.

We compare the beamforming and diversity configurations in Fig. 5 with the considered receiver structures. We can see that the performance of those two multiantenna configurations improves as we increase the number of antennas, and beamforming outperforms diversity. Note that the gain of performance obtained decreases as the number of antenna elements increases. It is better to use two antennas for this array system due to a reasonable tradeoff between performance and

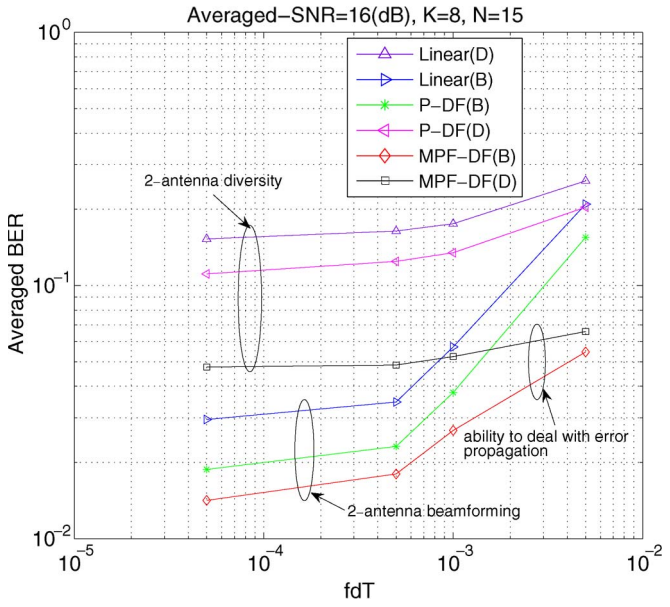

Fig. 6. BER performance versus channel fading rate for normalized SG algorithms, $N = 15$, $K = 8$ users, and two antennas for both diversity and beamforming configurations.

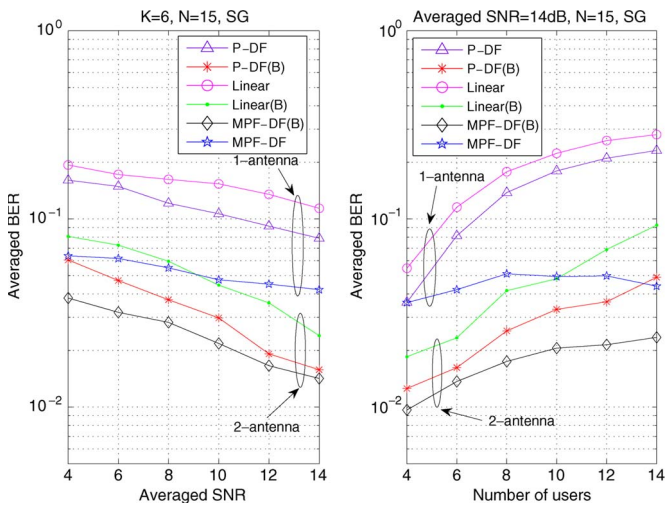

Fig. 7. BER performance versus (a) the averaged SNR and (b) the number of users K. Normalized SG algorithms, with $N = 15$, $f_dT = 5 \times 10^{-5}$, and two antennas for beamforming configurations.

complexity. This experiment is based on a channel with fading rate $f_dT = 1 \times 10^{-3}$.

In Fig. 6, we illustrate the performance of the following algorithms as the fading rate of the channel varies: linear, P-DF, MPF-DF combining diversity, and beamforming configurations. First, we can see that, as the fading rate increases, the performance gets worse, and our proposed space-time MPF-DF receivers outperform the existing schemes. Moreover, we observe that beamforming is better than diversity. Second, Fig. 6 shows the ability of the novel adaptive MPF-DF to deal with error propagation and channel uncertainties. The novel MPF-DF structure using beamforming performs best. The experiments of Figs. 5 and 6 employ Gold sequences with $N = 15$ as the spreading codes.

The next scenario, as shown in Fig. 7, considers the comparison in terms of the BER of the proposed DF structures, i.e.,

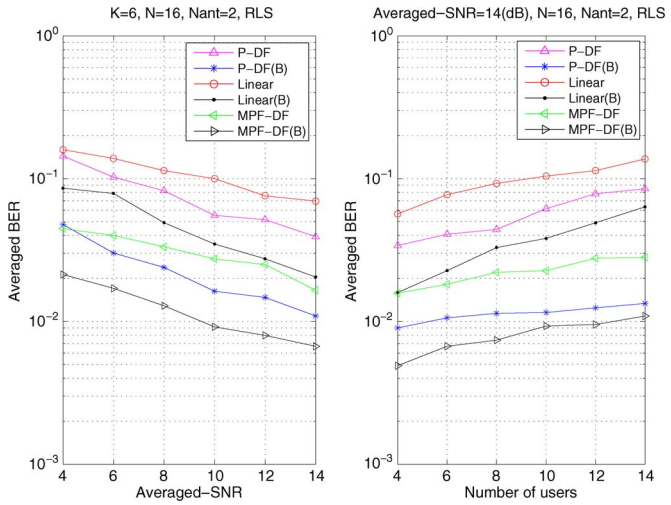

Fig. 8. BER performance versus (a) the average SNR and (b) the number of users K. RLS algorithms, with $N = 16$, $f_dT = 5 \times 10^{-5}$, and two antennas ($N_{\text{ant}} = 2$) for beamforming configurations.

the MPF-DF and MPF-DF combining beamforming technique with existing detectors for uncoded systems. Here, we use Gold sequences with $N = 15$ as spreading codes, and the normalized SG algorithms are employed to update the feedforward and feedback filters. In particular, we show the averaged BER performance curves versus the averaged SNR and number of users K for the analyzed receivers. The results in Fig. 7 indicate that the best performance is achieved with the novel MPF-DF with beamforming technique, followed by the P-DF receiver with beamforming, the linear with beamforming, the MPF-DF, the P-DF, and the linear receiver with a single antenna. Specifically, the MPF-DF with beamforming receiver can save up to 2 dB and support up to three more users, in comparison with the P-DF with beamforming for the same performance. It can substantially increase the system capacity. In this experiment, channel fading rate f_dT is equal to 5×10^{-5}.

The results for a system with $N = 16$ are shown in Fig. 8. The system employs RLS algorithms to estimate the values of feedforward and feedback filters; we use random sequences as the spreading codes. In particular, the same BER performance hierarchy is observed for the detection schemes, i.e., the MPF-DF, MPF-DF with beamforming, P-DF, P-DF with beamforming, linear receiver, and linear receiver with beamforming schemes. Comparing the curves obtained with the normalized SG algorithms in Fig. 7, we notice that the detection schemes with RLS algorithms outperform those with normalized SG algorithms and that there are also some additional gains in the performance for the proposed schemes over the existing techniques. Specifically, the MPF-DF detector can save up to 8 dB and support up to ten additional users, in comparison with the P-DF for the same BER performance based on RLS algorithms. Regarding the two-antenna combined beamforming configurations, the MPF-DF with beamforming scheme can save up to 5 dB and support up to six users, in comparison with the P-DF with beamforming for the same BER performance based on RLS algorithms. In the experiment, the channel fading rate is $f_dT = 5 \times 10^{-5}$.

The last scenario, as shown in Fig. 9, considers the experiments of our proposed space-time MPF-DF receiver structure

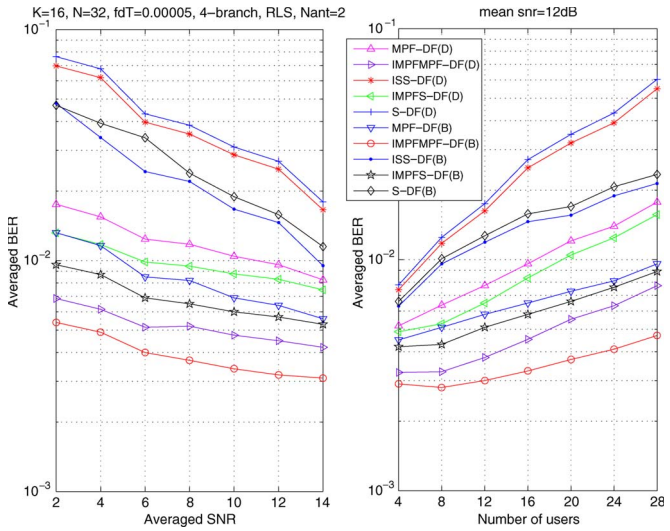

Fig. 9. BER performance versus (a) the average SNR and (b) the number of users K. RLS algorithms, with $N = 32$, $f_dT = 5 \times 10^{-5}$, and two antennas ($N_{\text{ant}} = 2$) for diversity and beamforming configurations.

equipped with two-antenna diversity and beamforming configurations combined with iterative cascaded DF stages. We compare the performance in terms of the BER of the proposed DF structures, i.e., MPF-DF, IMPFS-DF, and IMPFMPF-DF employing diversity and beamforming techniques with existing iterative and conventional DF for uncoded systems. In particular, we show the BER performance curves versus the averaged SNR and number of users K for the analyzed receivers. The systems use $N = 32$ random sequences as the spreading codes, and we employ the RLS algorithms to estimate the values of the feedforward and feedback filters for the first and second stages. The channel fading rate is $f_dT = 5 \times 10^{-5}$. The results shown in Fig. 9 indicate that the best performance is achieved with the novel IMPFMPF-DF with beamforming, followed by the new IMPFMPF-DF with diversity, the IMPFS-DF with beamforming, the MPF-DF with beamforming, the IMPFS-DF with diversity, the MPF-DF with diversity, the existing ISS-DF with beamforming, the S-DF with beamforming, the ISS-DF with diversity, and the S-DF with diversity. Specifically, the IMPFMPF-DF detector with beamforming can save up to more than 10 dB and support up to 20 more users, in comparison with the existing ISS-DF with beamforming for the same BER performance. The IMPFS-DF with beamforming scheme can save up to 8 dB and support up to 16 more users, in comparison with the ISS-DF with beamforming scheme for the same BER performance. Moreover, the performance advantages of the IMPFMPF-DF and IMPFS-DF using diversity and beamforming techniques are substantially superior to the other existing approaches.

VIII. Conclusion

In this paper, we have discussed the low-complexity near-optimal ordering algorithms and compared the results of diversity and beamforming configurations for array systems. A novel MPF-DF receiver with diversity and beamforming techniques for DS-CDMA systems and two adaptive algorithms have been proposed. The proposed schemes have also been combined with the iterative cascaded DF stages. It has been shown that the new detection schemes significantly outperform existing DF and linear receivers, support systems with higher loads, and mitigate the phenomenon of error propagation. It is worth noting that our proposed algorithms can also be extended to take into account coded systems, MC-CDMA systems, and other types of communications systems.

Appendix A
Analysis of Beamforming and Diversity Configurations

In this section, we study the beamforming and diversity configurations and analyze the advantages and disadvantages of each configuration. In particular, we focus our analysis on linear detectors for simplicity and resort to the SINR. It should be remarked that this analysis can be extended to other detectors, and the main results have been verified by simulations.

In Section II, we introduced the system model and gave the received vector in (4). Here, let us recall the stacking effective spreading code for the kth user, which is given by

$$\begin{aligned}\mathbf{p}_k &= \left[\widetilde{\mathbf{p}}_{k,1}^T, \widetilde{\mathbf{p}}_{k,2}^T, \ldots, \widetilde{\mathbf{p}}_{k,J}^T\right]^T \\ &= \left[(\mathbf{C}_k\mathbf{h}_{1,k})^T, (\mathbf{C}_k\mathbf{h}_{2,k})^T, \ldots, (\mathbf{C}_k\mathbf{h}_{J,k})^T\right]^T. \end{aligned} \tag{51}$$

For linear detectors with antenna arrays, the SINR of the desired user k_0 is computed as the ratio between the desired symbol energy and the energy of the interference plus noise

$$\begin{aligned}&\text{SINR}^{(k_0)} \\ &= \frac{E\left[\mathbf{w}^H\mathbf{p}_{k_0}b_{k_0}(i)b_{k_0}^*(i)\mathbf{p}_{k_0}^H\mathbf{w}\right]}{E\left[\mathbf{w}^H\left(\sum_{k\neq k_0}^K \mathbf{p}_k b_k(i)b_k^*(i)\mathbf{p}_k^H + \mathbf{n}(i)\mathbf{n}^H(i)\right)\mathbf{w}\right]} \\ &= \frac{\mathbf{w}^H\mathbf{p}_{k_0}\mathbf{p}_{k_0}^H\mathbf{w}}{\mathbf{w}^H\left(\sum_{k\neq k_0}^K \mathbf{p}_k\mathbf{p}_k^H + \sigma^2\mathbf{I}\right)\mathbf{w}} \end{aligned} \tag{52}$$

where filtering vector $\mathbf{w}$ is the linear detector, e.g., the MMSE detector $\mathbf{w} = (\sum_{k=1}^K \mathbf{p}_k\mathbf{p}_k^H + \sigma^2\mathbf{I})^{-1}\mathbf{p}_{k_0}$ or the Rake detector $\mathbf{w} = \mathbf{p}_{k_0}$. The matrices $\mathbf{p}_k\mathbf{p}_k^H$ in (52) for each k is developed as (53), shown at the bottom of the page, where $k = 1, \ldots, K$.

$$\mathbf{p}_k\mathbf{p}_k^H = \begin{pmatrix} \mathbf{C}_k\mathbf{h}_{1,k}\mathbf{h}_{1,k}^H\mathbf{C}_k^H & \mathbf{C}_k\mathbf{h}_{1,k}\mathbf{h}x_{2,k}^H\mathbf{C}_k^H & \ldots & \mathbf{C}_k\mathbf{h}_{1,k}\mathbf{h}_{J,k}^H\mathbf{C}_k^H \\ \mathbf{C}_k\mathbf{h}_{2,k}\mathbf{h}_{1,k}^H\mathbf{C}_k^H & \mathbf{C}_k\mathbf{h}_{2,k}\mathbf{h}_{2,k}^H\mathbf{C}_k^H & \ldots & \mathbf{C}_k\mathbf{h}_{2,k}\mathbf{h}_{J,k}^H\mathbf{C}_k^H \\ \vdots & \vdots & \ddots & \vdots \\ \mathbf{C}_k\mathbf{h}_{J,k}\mathbf{h}_{1,k}^H\mathbf{C}_k^H & \mathbf{C}_k\mathbf{h}_{J,k}\mathbf{h}_{2,k}^H\mathbf{C}_k^H & \ldots & \mathbf{C}_k\mathbf{h}_{J,k}\mathbf{h}_{J,k}^H\mathbf{C}_k^H \end{pmatrix} \tag{53}$$

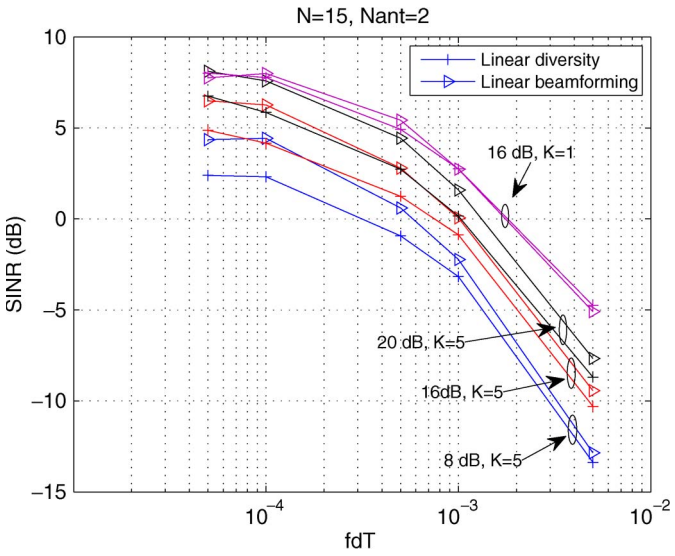

Fig. 10. Linear MMSE detector combing beamforming and diversity.

In the case of beamforming, the channel vector corresponding to the βth antenna is given by

$$\mathbf{h}_{\beta,k} = \begin{pmatrix} h_{\beta,k,1} \\ h_{\beta,k,2} \\ \vdots \\ h_{\beta,k,L_p} \end{pmatrix} = \begin{pmatrix} h_{1,k,1}e^{-j\phi_1(\beta-1)} \\ h_{1,k,2}e^{-j\phi_2(\beta-1)} \\ \vdots \\ h_{1,k,L_p}e^{-j\phi_{L_p}(\beta-1)} \end{pmatrix} \tag{54}$$

where $\beta = 1, \ldots, J$, and phase ϕ_l corresponds to the lth $(l = 1, \ldots, L_p)$ path of the kth user, which was introduced in Section II. The quantity $\mathbf{h}_{\beta,k}\mathbf{h}_{\gamma,k}^H$ in (53) is given by (55), shown at the bottom of the page, where $\gamma = 1, \ldots, J$; we can see the SINR of the beamforming case is a function of the DOAs and the fading gains.

For diversity, the channel vector of the βth antenna is $\mathbf{h}_{\beta,k} = [\alpha_{\beta,k,1}, \alpha_{\beta,k,2}, \ldots, \alpha_{\beta,k,L_p}]^T$, where the channel coefficients are uncorrelated. Thus, quantity $\mathbf{h}_{\beta,k}\mathbf{h}_{\gamma,k}^H$ is given by

$$\begin{pmatrix} \alpha_{\beta,k,1}\alpha_{\gamma,k,1}^* & \alpha_{\beta,k,1}\alpha_{\gamma,k,2}^* & \cdots & \alpha_{\beta,k,1}\alpha_{\gamma,k,L_p}^* \\ \alpha_{\beta,k,2}\alpha_{\gamma,k,1}^* & \alpha_{\beta,k,2}^*\alpha x_{\gamma,k,2}^* & \cdots & \alpha_{\beta,k,2}\alpha_{\gamma,k,L_p}^* \\ \vdots & \vdots & \ddots & \vdots \\ \alpha_{\beta,k,L_p}\alpha_{\gamma,k,1}^* & \alpha_{\beta,k,L_p}\alpha_{\gamma,k,2}^* & \cdots & \alpha_{\beta,k,L_p}\alpha_{\gamma,k,L_p}^* \end{pmatrix} \tag{56}$$

where the SINR of the diversity case is a function of the uncorrelated fading gains.

Fig. 10 shows that the SINR varies with the channel fading rate f_dT over the linear MMSE detector combining beamforming and diversity. We can see that, for the single-user case, the curves of these two configurations are very close, and the diversity configuration has a slightly better performance for higher fading rates. For the multiuser scenario, the beamforming outperforms the diversity, and the curves get close as the fading rate increases.

The beamforming technique spatially separates signals, because the information from different antenna elements is combined in such a way that the expected pattern of radiation is preferentially observed. Spatial diversity is an effective method for combating fading. Based on the discussion before, we can see that the detector combining beamforming will perform best in the case of a high number of users and slow fading environments. In situations with low number of users and severe fading environments, diversity combining should be employed. Note that diversity can be combined with beamforming to achieve better performance; in this case, each of the diversity branches consists of a number of beamforming elements [18].

Appendix B
On the MMSE With Perfect and Imperfect Feedback for the Proposed Space-Time MPF-DF Detectors

The proposed space-time MPF-DF employs multiple branches in parallel and chooses the best estimate among these parallel branches. First, let us consider the imperfect-feedback case. As we discussed in Section V, the feedforward and feedback filters for branch β of user k are

$$\mathbf{w}_{\beta,k} = \mathbf{R}^{-1}(\mathbf{p}_k + \mathbf{B}\mathbf{f}_{\beta,k}) \tag{57}$$

$$\mathbf{f}_{\beta,k} = \left(E\left[\hat{\mathbf{b}}_\beta \hat{\mathbf{b}}_\beta^H\right]\right)^{-1}\mathbf{B}^H\mathbf{w}_{\beta,k} \approx \mathbf{B}^H\mathbf{w}_{\beta,k}. \tag{58}$$

Substituting (57) and (58) into (18), we obtain the associated MMSE corresponding to branch β, i.e.,

$$\begin{aligned} J_{\mathrm{MMSE},\beta} \approx{}& \sigma_b^2 - (\mathbf{p}_k + \mathbf{B}\mathbf{f}_{\beta,k})^H\mathbf{R}^{-1}\mathbf{p}_k \\ & - \mathbf{p}_k^H\mathbf{R}^{-1}(\mathbf{p}_k + \mathbf{B}\mathbf{f}_{\beta,k}) \\ & + (\mathbf{p}_k + \mathbf{B}\mathbf{f}_{\beta,k})^H\mathbf{R}^{-1}(\mathbf{p}_k + \mathbf{B}\mathbf{f}_{\beta,k}) \\ & - (\mathbf{p}_k + \mathbf{B}\mathbf{f}_{\beta,k})^H\mathbf{R}^H\mathbf{B}\mathbf{f}_{\beta,k} \\ \approx{}& \sigma_b^2 - \mathbf{p}_k^H\mathbf{R}^{-1}\mathbf{p}_k - \mathbf{p}_k^H\mathbf{R}^{-1}\mathbf{B}\mathbf{f}_{\beta,k} \end{aligned} \tag{59}$$

where $\beta = 1, 2, \ldots, B$, with B being the number of branches. Therefore, the MMSE of the proposed MPF-DF for user k is approximately given by

$$J'_{\mathrm{MMSE}} \approx \min_{\{\beta\in 1,\ldots,B\}} \left(\sigma_b^2 - \mathbf{p}_k^H\mathbf{R}^{-1}\mathbf{p}_k - \mathbf{p}_k^H\mathbf{R}^{-1}\mathbf{B}\mathbf{f}_{\beta,k}\right). \tag{60}$$

Regarding the case of perfect feedback, let us divide the users into two sets, similarly to [9], i.e.,

$$D = \{j : \hat{b}_j \quad \text{is fed back}\} \tag{61}$$

$$U = \{j : j \notin D\} \tag{62}$$

$$\begin{pmatrix} |h_{1,k,1}|^2 e^{j\phi_1(\gamma-\beta)} & h_{1,k,1}h_{1,k,2}^* e^{j[\phi_2(\gamma-1)-\phi_1(\beta-1)]} & \cdots & h_{1,k,1}h_{1,k,L_p}^* e^{j\left[\phi_{L_p}(\gamma-1)-\phi_1(\beta-1)\right]} \\ h_{1,k,2}h_{1,k,1}^* e^{j[\phi_1(\gamma-1)-\phi_2(\beta-1)]} & |h_{1,k,2}|^2 e^{j\phi_2(\gamma-\beta)} & \cdots & h_{1,k,2}h_{1,k,L_p}^* e^{j\left[\phi_{L_p}(\gamma-1)-\phi_2(\beta-1)\right]} \\ \vdots & \vdots & \ddots & \vdots \\ h_{1,k,L_p}h_{1,k,1}^* e^{j\left[\phi_1(\gamma-1)-\phi_{L_p}(\beta-1)\right]} & h_{1,k,L_p}h_{1,k,2}^* e^{j\left[\phi_2(\gamma-1)-\phi_{L_p}(\beta-1)\right]} & \cdots & |h_{1,k,L_p}|^2 e^{j\phi_{L_p}(\gamma-\beta)} \end{pmatrix} \tag{55}$$

where the two sets D and U correspond to detected and undetected users, respectively. Here, we define matrices $\mathbf{P}_D = [\mathbf{p}_1, \ldots, \mathbf{p}_D]$ and $\mathbf{P}_U = [\mathbf{p}_1, \ldots, \mathbf{p}_U]$, and $\mathbf{R}_U = \mathbf{P}_U\mathbf{P}_U^H + \sigma^2\mathbf{I} = \mathbf{R} - \mathbf{P}_D\mathbf{P}_D^H$. Covariance matrices $\mathbf{R}_D$ and $\mathbf{R}_U$ change with different branches. Let us consider the perfect-feedback case, i.e., $\hat{\mathbf{b}}_\beta(i) = \mathbf{b}_\beta(i)$. Note that the DF receivers based on the imperfect feedback depend on matrix $\mathbf{B} = E[\mathbf{r}(i)\hat{\mathbf{b}}_\beta^H(i)]$, which, under perfect feedback, is equal to $\mathbf{P}_{D_\beta}$. Following the same approach, we have the feedforward and feedback filters as

$$\mathbf{w}_{\beta,k} = \mathbf{R}_{U_\beta}^{-1}\mathbf{p}_k \tag{63}$$

$$\mathbf{f}_{\beta,k} = \mathbf{P}_{D_\beta}^H\mathbf{w}_{\beta,k}. \tag{64}$$

Substituting (63) and (64) into (18), we obtain the associated MMSE corresponding to branch β

$$J_{\mathrm{MMSE},\beta} = \sigma_b^2 - \mathbf{p}_k^H\mathbf{R}_{U_\beta}^{-1}\mathbf{p}_k \tag{65}$$

where covariance matrix $\mathbf{R}_{U_\beta}$ corresponds to the set of undetected users and changes with different branches. Similarly, we obtain the MMSE for MPF-DF detectors in the perfect-feedback case

$$J'_{\mathrm{MMSE}} \approx \min_{\{\beta\in 1,\ldots,B\}} \left(\sigma_b^2 - \mathbf{p}_k^H\mathbf{R}_{U_\beta}^{-1}\mathbf{p}_k\right). \tag{66}$$

Appendix C
On the MMSE With Perfect and Imperfect Feedback for S-DF and P-DF With Antenna Arrays

The conventional S-DF detector with antenna arrays can be treated as a special case of the proposed space-time MPF-DF detector (with $B = 1$). We have quite similar equations of the feedforward and feedback filters, as we discussed before; here, we focus on the perfect-feedback case for simplicity. The MMSE of the multiantenna S-DF detector is

$$J_{\mathrm{MMSE}} = \sigma_b^2 - \mathbf{p}_k^H\mathbf{R}_U^{-1}\mathbf{p}_k \tag{67}$$

where $\mathbf{p}_k$ is a stack of the effective spreading sequence regarding different antennas.

Specifically, for the P-DF detector with antenna arrays, we have

$$D = \{1, \ldots, k-1, k+1, \ldots, K\} \quad U = \{k\} \tag{68}$$

since D is a single cell; therefore, the MMSE associated with the space-time P-DF can be simplified by substituting $\mathbf{R}_U = \mathbf{p}_k\mathbf{p}_k^H + \sigma^2\mathbf{I}$ into (67), which yields

$$J_{\mathrm{MMSE}} = \sigma_b^2 - \mathbf{p}_k^H\left(\mathbf{p}_k\mathbf{p}_k^H + \sigma^2\mathbf{I}\right)^{-1}\mathbf{p}_k. \tag{69}$$

References

[1] M. L. Honig and H. V. Poor, "Adaptive interference suppression," in *Wireless Communications: Signal Processing Perspectives*, H. V. Poor and G. W. Wornell, Eds. Englewood Cliffs, NJ: Prentice-Hall, 1998, ch. 2, pp. 64–128.

[2] S. Verdu, *Multiuser Detection*. Cambridge, U.K.: Cambridge Univ. Press, 1998.

[3] S. Verdu, "Minimum probability of error for asynchronous Gaussian multiple-access channels," *IEEE Trans. Inf. Theory*, vol. IT-32, no. 1, pp. 85–96, Jan. 1986.

[4] R. Lupas and S. Verdu, "Linear multiuser detectors for synchronous code-division multiple-access channels," *IEEE Trans. Inf. Theory*, vol. 35, no. 1, pp. 123–136, Jan. 1989.

[5] M. Abdulrahman, A. Sheikh, and D. D. Falconer, "Decision feedback equalization for CDMA in indoor wireless communications," *IEEE J. Sel. Areas Commun.*, vol. 12, no. 4, pp. 698–706, May 1994.

[6] P. Patel and J. Holtzman, "Analysis of a simple successive interference cancellation scheme in a DS/CDMA systems," *IEEE J. Sel. Areas Commun.*, vol. 12, no. 5, pp. 796–807, Jun. 1994.

[7] M. K. Varanasi and B. Aazhang, "Multistage detection in asynchronous CDMA communications," *IEEE Trans. Commun.*, vol. 38, no. 4, pp. 509–519, Apr. 1990.

[8] P. B. Rapajic, M. L. Honig, and G. K. Woodward, "Multiuser decision-feedback detection: Performance bounds and adaptive algorithms," in *Proc. IEEE Int. Symp. Inf. Theory*, Boston, MA, Aug. 1998, p. 34.

[9] G. Woodward, R. Ratasuk, M. L. Honig, and P. B. Rapajic, "Minimum mean-square error multiuser decision-feedback detectors for DS-CDMA," *IEEE Trans. Commun.*, vol. 50, no. 12, pp. 2104–2112, Dec. 2002.

[10] M. L. Honig, G. K. Woodward, and Y. Sun, "Adaptive iterative multiuser decision feedback detection," *IEEE Trans. Wireless Commun.*, vol. 3, no. 2, pp. 477–485, Mar. 2004.

[11] J. E. Smee and S. C. Schwartz, "Adaptive space-time feedforward/feedback detection for high data rate CDMA in frequency-seletive fading," *IEEE Trans. Commun.*, vol. 49, no. 2, pp. 317–328, Feb. 2001.

[12] M. K. Varanasi and T. Guess, "Optimum decision feedback multiuser equalization with successive decoding achieves the total capacity of the Gaussian multiple-access channel," in *Proc. 31st Asilomar Conf. Signals, Syst. Comput.*, Monterey, CA, Nov. 1997, pp. 1405–1409.

[13] A. Duel-Hallen, "A family of multiuser decision-feedback detectors for asynchronous code-division multiple-access channels," *IEEE Trans. Commun.*, vol. 43, no. 234, pp. 421–434, Feb.–Apr. 1995.

[14] R. C. de Lamare and R. Sampaio-Neto, "Minimum mean squared error iterative successive parallel arbitrated decision feedback detectors for DS-CDMA systems," *IEEE Trans. Commun.*, vol. 56, no. 5, pp. 778–789, May 2008.

[15] A. Yener, R. D. Yates, and S. Ulukus, "Combined multiuser detection and beamforming for CDMA systems: Filter structures," *IEEE Trans. Veh. Technol.*, vol. 51, no. 5, pp. 1087–1095, Sep. 2002.

[16] G. Barriac and U. Madhow, "PASIC: A new paradigm for low-complexity multiuser detection," in *Proc. Conf. Inf. Sci. Syst.*, Mar. 21–23, 2001.

[17] S. Haykin, *Adaptive Filter Theory*, 4th ed. Englewood Cliffs, NJ: Prentice-Hall, 2002.

[18] P. V. Rooyen, M. Lotter, and D. V. Wyk, *Space-Time Processing for CDMA Mobile Communications*. Norwell, MA: Kluwer, 2001.

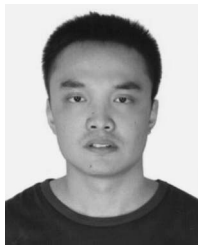

Yunlong Cai received the B.S. degree in computer science from Beijing Jiaotong University, Beijing, China, in 2004 and the M.Sc. degree in electronic engineering from the University of Surrey, Guildford, U.K., in 2006. He is currently working toward the Ph.D. degree with the Communications Research Group, Department of Electronics, University of York, York, U.K.

His research interests include spread-spectrum communications, adaptive signal processing, multiuser detection, and multiple-antenna systems.

Rodrigo C. de Lamare (S'99–M'04) received the Diploma degree in electronic engineering from the Federal University of Rio de Janeiro (UFRJ), Rio de Janeiro, Brazil, in 1998 and the M.Sc. and Ph.D. degrees in electrical engineering from the Pontifical Catholic University of Rio de Janeiro (PUC-Rio), in 2001 and 2004, respectively.

From January 2004 to June 2005, he was a Postdoctoral Fellow with the Center for Studies in Telecommunications, PUC-Rio. From July 2005 to January 2006, he was a Postdoctoral Fellow with the Signal Processing Laboratory, UFRJ. Since January 2006, he has been with the Communications Research Group, Department of Electronics, University of York, York, U.K., where he is currently a Lecturer of communications engineering. His research interests are communications and signal processing.